

A general model for the propagation of uncertainty in measurements into heat transfer simulations and its application to cryosurgery[☆]

Yoed Rabin*

Department of Mechanical Engineering, Carnegie Mellon University, Pittsburgh, PA 15213, USA

Received 25 October 2002; accepted 14 January 2003

Abstract

This report presents a technique for estimating the propagation of uncertainty in measurements into mathematical simulations of heat transfer. The motivation for this report is to show the dramatic uncertainty associated with estimating the value of the so-called “lethal temperature,” even in a case where a perfect correlation appears to exist between histopathologic observations and a corresponding heat transfer simulation. Although the example presented in this report relates to cryosurgery, the technique proposed in this report is rather general and can be applied to any heat transfer problem. The uncertainty analysis presented in this report can be considered as an extension of the well-known concept of the rule of the square root of the sum of the square errors. A comparison of the new technique with the worst case scenario concept is also presented. In conclusion, it is recommended that the proposed technique be routinely applied when presenting simulated results, whether as a part of a theoretical study, or in comparison with experimental data.

© 2003 Elsevier Science (USA). All rights reserved.

Keywords: Bioheat transfer; Uncertainty; Thermal analysis; Cryosurgery; Lethal temperature

A principle concept in experimental engineering is that no measurement can be taken without error. Hence, neither the exact value of the quantity being measured, nor the exact error associated with the measurement can be ascertained. In engineering, as in biology, the uncomfortable principle of indeterminacy exists. While uncertainties may be associated with an inaccurate experimental work performed in a less-than-perfect world, un-

certainities can be very useful and, like friction, are often a blessing in disguise. It is common practice to report on experimental data with an estimation of uncertainty. However, when experimental data are applied to mathematical analyses of bioheat transfer, experimental uncertainties are typically ignored, and only average values are taken into consideration. Hence, the propagation of uncertainty in measurements into the mathematical solution is typically overlooked.

The solved parameter in a bioheat transfer problem is most frequently the transient temperature distribution. In a freezing/thawing problem,

[☆] This work was funded by institutional sources.

* Fax: 1-412-268-3348.

E-mail address: rabin@cmu.edu

the solution also includes the location of a freezing/thawing front. Many parameters are involved in a mathematical solution of a bioheat transfer problem (the terms ‘mathematical solution’ and ‘mathematical simulation’ are synonymous in this context), and can generally be separated into four groups: (i) intrinsic physical properties, such as thermal conductivity, specific heat, density, and latent heat; (ii) biological parameters, such as blood perfusion rate, metabolic heat generation, and core body temperature; (iii) geometrical parameters, including dimensions and orientation of the solved domain, as well as specific details on blood vessels, and ducts; and (iv) thermal boundary conditions, describing the driving mechanism of cooling and/or warming.

Mathematical solutions of bioheat transfer may be used for a large variety of purposes, such as theoretical studies, parametric estimation of physical properties, and analysis of experimental results [6,23]. Either way, the mathematical solution relies on a prior knowledge of some of the above parameters, each of which is associated with a unique level of uncertainty. Even when the uncertainty associated with each parameter is fairly estimated, estimating the level of uncertainty associated with the solved parameters—the temperature distribution, and possibly the freezing front location—remains a major challenge.

A common concept for estimating the propagation of measurement uncertainties into a mathematical solution is based on a worst case scenario analysis. Using this concept, parametric studies are performed based on sets of extreme parameter values, in order to bound the possible range in which the real solution is likely to exist [19,24]. While the concept of worst case scenario may be based on some rational arguments, there is no mathematical background for its support. In some cases, the worst case scenario concept may lead to an extremely high overestimation of uncertainty of the mathematical solution.

An alternative concept for estimating the propagation of measurement uncertainties into a mathematical solution is based on Monte Carlo simulations [11]. Using this concept, the mathematical solution is repeated many times, each time using a randomly selected set of parameter values,

where the interval for random selection of each parameter is its range of uncertainty. Statistical analysis of such a large number of mathematical solutions provides the range in which the real solution is likely to exist; this is the uncertainty interval of the solution. The same statistical analysis also provides a probability distribution of the uncertainty, which indicates the likelihood of finding the real solution at any given point within the uncertainty interval. In general, the Monte Carlo analysis requires many simulations and therefore is very expensive.

The purpose of the current report is to present a third concept for estimating the propagation of measurement uncertainties into a mathematical solution of bioheat transfer. This concept leads to a straightforward technique, which is far less expensive than the Monte Carlo technique. The new concept relies on statistical principles, however, no actual statistical work is required. This report includes a method for the application of the new concept with examples related to cryosurgery and *in vivo* measurements of the lethal temperature. Nevertheless, the technique can be applied to any heat transfer process.

The current report does not include uncertainty effects due to interaction between the sensor and the sensed phenomenon. In the context of cryobiology, this interaction results in heat conduction by sensors and instrumentation, which either elevate or decrease the temperature at the point of measurement [17,18].

Mathematical formulation of uncertainty

Analysis of uncertainty is required in order to evaluate the quality of experimental data, estimate the propagation of measurement uncertainties into a mathematical solution, or to evaluate the quality of empirical correlations. Techniques for evaluating the quality of experimental data are widely available in the literature, and are beyond the scope of the current report. A formulation for estimating the propagation of measurement uncertainties into a mathematical solution is presented below. Following is an expansion of the formulation for empirical correlations.

Uncertainty in mathematical simulations of bioheat transfer

Three elements are required in order to simulate heat transfer in a specific problem: (i) a thermal model of heat transfer, most commonly presented in the form of a differential equation (integral and lumped formulations are well-established alternatives); (ii) a numerical technique for translating the thermal model into a numerical scheme; and (iii) a list of numerical values for all the thermal model parameters, as listed in the introduction.

Modeling of a physical problem with mathematical equations is associated with some level of uncertainty. For example, there were at least five generations of modeling of bioheat transfer [3,5]. After the first model, widely known as “the classical bioheat equation” [14], new models were offered to decrease the level of model uncertainty. Comparison of uncertainty between different models can only be done based on observations made on a specifically designed experimental setup [3,5], which is beyond the scope of the current report.

Translating the physical model into a numerical solution is also associated with some level of uncertainty. In broad terms, this uncertainty results from numerical discretization of the mathematical model, stability and convergence of the solution, and round off errors in computer calculations. Software compilers and computer hardware can also contribute to uncertainty in mathematical simulations. Analysis of uncertainty in numerical schemes are widely available in the literature [2], and are routinely presented with reports on new numerical schemes. Uncertainty analysis of specific numerical techniques is beyond the aims of the current report. Nevertheless, the discussion section of the current report includes a comparison of uncertainty due to numerical simulations with uncertainty due to propagation of measurement uncertainties into a mathematical solution.

Consistent with the above arguments, it is assumed in the current report that the thermal model and the numerical scheme are established. In general, the solution for the temperature distribution at a specific time can be presented as a function of all of the model parameters:

$$\begin{aligned} T &= f(p_1, p_2, \dots, p_i, \dots, p_n) \\ &= f(k, C, L, q_{\text{met}}, w, T_b), \end{aligned} \quad (1)$$

where T is the temperature solution, f is a function, p_i is a representative parameter, and n is the total number of relevant model parameters. For demonstration purposes, the following set of relevant parameters is assumed (also included in Eq. (1)): k is the thermal conductivity, C is the volumetric specific heat, L is the latent heat of phase transition, q_{met} is the metabolic heat generation, w is the blood perfusion rate, and T_b is the blood temperature.

The value of each parameter is assumed to be independently associated with some uncertainty interval δ . This uncertainty interval is frequently reported in scientific reports on experimental work, and is assumed to be known when the heat transfer problem is solved. The only unknown uncertainty is that of the calculated temperature distribution:

$$\begin{aligned} T \pm \delta T &= f(p_1 \pm \delta p_1, p_2 \pm \delta p_2, \dots, \\ &\quad p_i \pm \delta p_i, \dots, p_n \pm \delta p_n) \\ &= f(k \pm \delta k, C \pm \delta C, L \pm \delta L, \\ &\quad q_{\text{met}} \pm \delta q_{\text{met}}, w \pm \delta w, T_b \pm \delta T_b). \end{aligned} \quad (2)$$

Estimation of the level of uncertainty in temperature, δT , is the motivation for developing the current formulation. Assuming that each δ represents a small interval, a Taylor expansion series of a first order can be written for the temperature:

$$\begin{aligned} T \pm \delta T &= f + \sum_{i=1}^n \left(\pm \frac{\partial f}{\partial p_i} \delta p_i \right) \\ &= f \pm \frac{\partial f}{\partial k} \delta k \pm \frac{\partial f}{\partial C} \delta C \pm \frac{\partial f}{\partial L} \delta L \\ &\quad \pm \frac{\partial f}{\partial q_{\text{met}}} \delta q_{\text{met}} \pm \frac{\partial f}{\partial w} \delta w \pm \frac{\partial f}{\partial T_b} \delta T_b. \end{aligned} \quad (3)$$

When the solution for T is linearly dependent on p_i , Eq. (3) holds, even when δ is not small. In the case when the uncertainty interval δp_i is of the same order as of property p_i , and when T is not linearly dependent on p_i , a higher order Taylor expansion is required than that presented in Eq. (3). On the other hand, estimating the uncertainty

in temperature when δp_i is of the same order as of p_i requires further discussion and is addressed below. Since T and f are identical, Eq. (3) can be reduced to:

$$\begin{aligned} \pm \delta T &= \sum_{i=1}^n \left(\pm \frac{\partial f}{\partial p_i} \delta p_i \right) \\ &= \pm \frac{\partial f}{\partial k} \delta k \pm \frac{\partial f}{\partial C} \delta C \pm \frac{\partial f}{\partial L} \delta L \pm \frac{\partial f}{\partial q_{\text{met}}} \delta q_{\text{met}} \\ &\quad \pm \frac{\partial f}{\partial w} \delta w \pm \frac{\partial f}{\partial T_b} \delta T_b. \end{aligned} \quad (4)$$

Since each term in Eq. (4) can have either a minus or a plus sign, accounting for the combined effect of all of these uncertainties may not be obvious. To calculate the maximum possible uncertainty in temperature, one may take the worst case scenario, where all signs are identical. An alternative way to estimate the magnitude of δT in Eq. (4), is based on a statistical approach [9]. For this purpose, assume that: (i) the probability of the real value of p_i to be within a range of $\pm \delta p_i$, centered around its estimated value, is known; (ii) the probability distribution of uncertainty is similar for all parameters (most frequently—*normal probability distribution*, addressed below); and (iii) all the parameters, p_i , are independent of each other. Under these assumptions, it can be shown that δT has a probability distribution similar to the uncertainty probability distribution of all of the primitive parameters, when δT is calculated as follows [9]:

$$\delta T = \sqrt{\sum_{i=1}^n \left(\frac{\partial f}{\partial p_i} \delta p_i \right)^2}. \quad (5)$$

Eq. (5) is known as the rule of the square root of the sum of the square errors, and is often used to analyze uncertainty in experimental systems. To the best of this author's knowledge, Eq. (5) has never before been used to analyze uncertainty in mathematical solutions of bioheat transfer.

Gauss–Laplace *normal probability distribution* is most frequently observed in engineering measurements [9]. For normal distribution, the direct interpretation of the standard deviation, σ , is that 68.2% of all possible values of p_i will fall within the

$\pm \sigma$ interval, centered on the average value. Similarly, 95.5% of all possible values of p_i will fall within the $\pm 2\sigma$ interval, centered on the average value. For any engineering application, $\pm \sigma$ interval is not good enough, and a wider interval must be employed to express greater confidence, where the probability that an individual measurement will fall outside of the uncertainty interval is typically 1:20 (corresponds to 1.96σ). The value of δ in reports on experimental work is typically σ . Normal probability distribution of uncertainties is assumed for all parameters in the current report, and δ is assumed to be 2σ .

While Eqs. (1)–(5) present a well-established approach of uncertainty formulation, the outstanding question is how to incorporate this formulation into a numerical solution of a bioheat transfer problem. For the purpose of discussion, it is assumed that heat transfer in biological tissues can be modeled by the classical bioheat equation [14]:

$$\rho \frac{\partial T}{\partial t} = \nabla \cdot (k \nabla T) + w_b C_b (T_b - T) + q_{\text{met}}, \quad (6)$$

where t is time. It is further assumed that a numerical solution for Eq. (6) is available.

The solution of Eq. (6) is a transient temperature distribution. The temperature solution at a specific location in space and at a specific point in time is:

$$T_0 \equiv T(x_1, x_2, x_3, t) = f(p_1, p_2, \dots, p_i, \dots, p_n), \quad (7)$$

where x_1 , x_2 , and x_3 are spatial coordinates and where average parameter values are used to generate the solution. Let another solution be obtained at the same location and time, using average values for all parameters with only one exception—the value of parameter i is taken as $p_i + \delta p_i$. The second solution is defined as:

$$\begin{aligned} T_i &\equiv T(x_1, x_2, x_3, t) \\ &= f(p_1, p_2, \dots, p_i + \delta p_i, \dots, p_n). \end{aligned} \quad (8)$$

Eq. (8) represents a series of n solutions, each with the variation of a different model parameter.

The partial derivatives in Eq. (5) can readily be obtained by:

$$\frac{\partial f}{\partial p_i} \delta p_i \cong \frac{T_i - T_0}{\Delta p_i} \delta p_i = [T_i - T_0]_{\Delta p_i = \delta p_i} \equiv \Delta T_i. \quad (9)$$

Note that, for simplicity, Δp_i was chosen to be equal to δp_i in the right two terms of Eq. (9).

Thus far the formulation has been presented for uncertainty in temperature, however, the solution in some bioheat transfer problem includes other parameters, such as interface location, and heat fluxes along specific boundaries. The mathematical treatment of uncertainty in these parameters of solution is identical to the uncertainty formulation for temperature, when the symbol T in Eqs. (1)–(5) and Eqs. (7)–(9) is replaced with the symbol representing the relevant parameter of the solution.

Uncertainty in experimental correlations

An experimental correlation is a mathematical description of a physical phenomenon based on experimental observations, and not on a theoretical model. A well-known empirical correlation in cryobiology is the relationship between the cooling rate during freezing and cell destruction [12]. A well-known empirical correlation in cryosurgery is the lethal temperature value for different organs, where the term “lethal temperature” refers to a temperature threshold below which maximum cell destruction is achieved [8]. Identifying the value of the lethal temperature, for example, is performed by comparing temperature measurements with histo-pathologic observations. However, since neither the lethal temperature value nor its location at the end of freezing are known a priori, a mathematical solution is required to correlate temperature at discrete points of measurement with the continuous temperature distribution. One of the objectives of the current report is to offer a systematic technique to estimate the uncertainty associated with estimations of the lethal temperature.

Uncertainty analysis of an empirical correlation can follow the rule of the square root of the sum of the square errors, Eq. (5), where the model parameters also include sensors in the system. The process of uncertainty analysis in this case follows the same procedure described in Eqs. (1)–(9). Extending the example presented in Eq. (4), and assuming that comparison of experimental data with computer simulations also includes uncertainty in temperature sensor localization and hardware,

the uncertainty in the computed temperature becomes:

$$\begin{aligned} \pm \delta T = & \pm \frac{\partial f}{\partial k} \delta k \pm \frac{\partial f}{\partial C} \delta C \pm \frac{\partial f}{\partial L} \delta L \\ & \pm \frac{\partial f}{\partial q_{\text{met}}} \delta q_{\text{met}} \pm \frac{\partial f}{\partial w} \delta w \pm \frac{\partial f}{\partial T_b} \delta T_b \\ & \pm \frac{\partial f}{\partial x_1} \delta x_1 \pm \frac{\partial f}{\partial x_2} \delta x_2 \pm \frac{\partial f}{\partial x_3} \delta x_3 \pm \frac{\partial f}{\partial T_e} \delta T_e, \quad (10) \end{aligned}$$

where T_e is an experimentally measured temperature used as an input for the mathematical solution, δT_e is temperature uncertainty due to hardware, and δx_i is uncertainty in location of analysis. A numerical example for experimental correlation is given in the discussion section.

Solution parameters

Thermophysical properties of biomaterials at the normal body temperature range are widely available in the literature [4]. However, data on thermophysical properties of biomaterials at cryogenic temperatures is very limited. In the absence of more specific knowledge, and as a first order approximation, thermophysical properties of pure ice are typically assumed for biomaterial. Typical ranges for the most common solution parameters are presented below. This presentation is provided to develop a sense of the corresponding uncertainty range, and to prepare the grounds for the numerical examples given below. However, by no means is this presentation meant to cover all available experimental data in detail.

Thermal conductivity. Thermal conductivity of pure ice can be approximated as [20]:

$$k = \frac{k_0}{T^m}, \quad (11)$$

where m and k_0 are constants; for pure ice: $m = 1.235$ and $k_0 = 2135 \text{ W/m K}^{1-m}$, and for blood: $m = 1.15$ and $k_0 = 1005 \text{ W/m K}^{1-m}$. Thermal conductivity range for pure ice, at some selected temperatures is presented in Fig. 1(a), compiled from eight experimental reports reviewed by Fukusako [7] and Rabin [20]. In the absence of uncertainty analysis in those early experimental

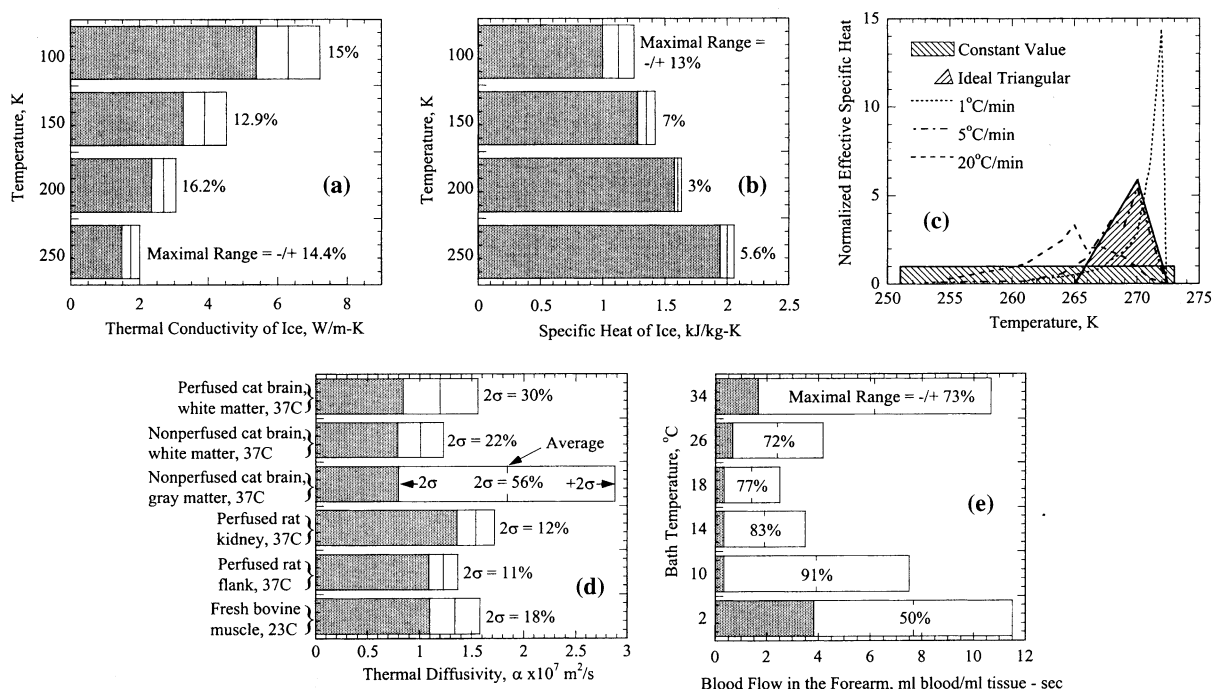


Fig. 1. Thermophysical properties and blood perfusion rate: (a) thermal conductivity range for pure ice, compiled from eight experimental reports reviewed by Fukusako [7] and Rabin [20]; (b) specific heat range of pure ice, compiled from six experimental reports reviewed by Fukusako [7]; (c) normalized effective specific heat compiled from experimental work on PBS by Smith et al. [24]; (d) thermal diffusivity distribution of biomaterials, measured by Newman and Lele [13]; and (e) blood flow in the forearm, compiled from experimental reports reviewed by Altman and Dittmer [1].

reports, the range in Fig. 1(a) is based on extreme values found in the literature and not on a specific uncertainty analysis.

Specific heat. Based on experimental observations [7], specific heat of pure ice can be approximated as:

$$C = 0.185 + 0.689 \times 10^{-2} \times T \quad \text{MJ/m}^3 \text{ K};$$

$$273 \text{ K} > T > 90 \text{ K},$$

$$C = 0.895 + 10^{-2} \times T \quad \text{MJ/m}^3 \text{ K};$$

$$90 \text{ K} > T > 40 \text{ K}.$$
(12)

The specific heat range for pure ice at some selected temperatures, is presented in Fig. 1(b), compiled from six experimental reports reviewed by Fukusako [7]. Similar to the presentation in Fig. 1(a), and in the absence of uncertainty analysis in those early experimental reports, the range in Fig. 1(b) is based on extreme values found in the literature. The specific heat of biomaterials in the frozen state, close to the lower boundary of phase

transition (i.e., -22°C), is typically in the range of 1.8 to 2 MJ/m³ K [4,16].

Latent heat. Latent heat of soft biological tissues is typically in the range of 250–333 MJ/m³ [10,24], where the upper boundary is the latent heat value of pure water. The latent heat is the enthalpy change of the material as a result of phase transition. In biological tissues, phase transition occurs over a relatively wide temperature range of up to 22°C (assuming that biological solutions can be first order approximated as an NaCl solution). For the purpose of mathematical simulations, it is very convenient to substitute the intrinsic property of latent heat with an effective property of specific heat, which is known as the “enthalpy approach.” The effective specific heat is chosen so that the integral of the effective specific heat over temperature, within the boundaries of phase transition, is equal to the value of the latent heat. The functional behavior of the latent heat can be chosen based on experimental observations,

or arbitrarily, as long as the latent heat value is preserved through the definition of the effective specific heat. Nonetheless, the mathematical solution is typically not sensitive to the choice of the functional behavior of the effective specific heat [15]. In experiments on phosphor-buffered solutions (PBS), Smith et al. [24] showed that the latent heat is strongly dependent on the cooling rate, a typically overlooked phenomenon. Fig. 1(c) presents two possible choices of the effective specific heat: (i) uniformly distributed value and (ii) an ideal triangular shape [19]. The effective specific heat scale is normalized with respect to the uniformly distributed effective specific heat. Also presented in Fig. 1(c) is the normalized effective specific heat of PBS, at various cooling rates, as compiled from Smith et al. [24]. A latent heat value $250 \text{ MJ/m}^3 \pm 2\%$ has been reported for all cooling rates by Smith et al. [24].

Thermal diffusivity: The thermal diffusivity of biomaterials at normal body temperatures is presented in Fig. 1(d) [13]. Reports on thermophysical properties of biomaterials at normal body temperature are comprehensive [4]. It can clearly be seen that the uncertainty range of thermal diffusivity may be very significant. In general, thermal conductivity and specific heat show similar uncertainty intervals, where thermal diffusivity is the ratio of the former to the latter. The thermal conductivity range of soft biological tissues (excluding fat) in normal body temperatures is typically in the range $0.39\text{--}0.58 \text{ W/m K}$, while specific heat is typically in the range $3\text{--}4 \text{ MJ/m}^3 \text{ K}$ [4]. Measurements of thermal conductivity and thermal diffusivity can be significantly affected by the rate of blood perfusion in the area of the measurements [25].

Blood perfusion: A comprehensive review of blood flow rates is given by Altman and Dittmer [1]. For example, Fig. 1(e) shows the range of possible average blood flow rate in the human forearm. The specific technique of measurement is based on immersing the limb in a water bath, momentarily blocking the central vein, and measuring the change of the water level in the bath. This measurement is translated into a value of the total flow rate of blood, which causes the change in water level. Fig. 1(e) offers an interesting oppor-

tunity to identify the dependency of blood temperature on the surrounding temperature (water in this case). More detail about this relationship can be found in [22]. Fig. 1(e) represents the typically high uncertainty associated with blood flow rate. Moreover, it is predicted that the maximal possible blood flow rate in internal organs can far exceed the values shown in Fig. 1(e) by an order of magnitude. It has been suggested by Shitzer [22] that the maximum possible blood flow can yield a heating effect of $40 \text{ kW/m}^3 \text{ K}$, where the latter is defined as the product of the blood flow rate and its volumetric specific heat ($w_b C_b$ in Eq. (6)).

Results and discussion

For the purpose of discussion, a typical numerical example of cryosurgery is given. The mathematical solution is of a 1D heat transfer problem around a cylindrical cryoprobe. The diameter of the cryoprobe is 1.5 mm . The cooling protocol is typical to a Joule-Thomson cryoprobe using Argon gas: cooling from 310 K (37°C) to 128 K (-145°C) in 30 s , and a constant temperature of 128 K thereafter [21]. Other solution parameters are listed in Table 1. Thermal conductivity of blood is assumed for soft tissues in the frozen state, an average thermal conductivity value of biomaterials is assumed in the unfrozen state, and a linear dependency of thermal conductivity in temperature is assumed in the phase transition range. Linear temperature dependency is assumed for specific heat in the cryogenic temperature range, starting from zero at absolute zero temperature and reaching a value of $1.9 \text{ MJ/m}^3 \text{ K}$ at the lower boundary of phase transition. A uniform effective specific heat is assumed in the phase transition temperature range, related to an average latent heat of 285 MJ/m^3 . An average specific heat value is assumed in the unfrozen region. The blood perfusion rate is typically the model parameter with the highest uncertainty in bioheat transfer simulations. One half of the maximum value is assumed as an average value with an uncertainty level of 100% . Clearly this is a large uncertainty interval, and the formulation presented above is valid only if at least one of the following conditions is met: (i) the effect

Table 1
Model parameters used for computer simulations

Parameter	Value	Uncertainty range (%)
Phase transition temperature range	$T_f = 251 \text{ K}$ to $T_u = 273 \text{ K}$	—
Thermal conductivity, W/m K	$k = \begin{cases} 1005 \times T^{-1.15}, & T < T_f, \\ 16.18 + 0.0575 \times T, & T_f < T < T_u, \\ 0.485, & T_u < T \end{cases}$	20
Specific heat, MJ/m ³ K	$C = \begin{cases} 7.57 \times 10^{-3} \times T, & T < T_f, \\ 12.95, & T_f < T < T_u, \\ 3.5, & T_u < T \end{cases}$	15
Blood heating effect, kW/m ³ K	$w_b C_b = 20$	100

of uncertainty in blood perfusion does not overwhelm the effects of other sources of uncertainty, or (ii) the uncertainty of the mathematical solution is linearly dependent on the uncertainty in blood perfusion. All numerical work in this study is based on the numerical scheme presented by Rabin and Shitzer [19] for cryosurgery simulations, which is based on a general numerical approach by Rabin and Korin [15].

The results of this numerical example are shown in Fig. 2. From Fig. 2(b) it can be seen that during the 10 min of simulation, the level of uncertainty does not change significantly with time in the frozen region. In the frozen region, uncertainty in temperature increases almost linearly with temperature, from 0 to 7 K at the lower boundary of phase transition temperature range. It can further

be seen that the maximal uncertainty in the unfrozen region is found at the upper boundary of the phase transition temperature range. The level of uncertainty in the unfrozen region increases almost linearly with time, from 12.2 K after 1 min (not shown in the figure), to 17 K after 10 min. Uncertainty within the phase transition temperature range is bounded by the maximum uncertainty values in the frozen and unfrozen regions.

Fig. 3 provides insight on the effect of each model parameter on the overall level of uncertainty. In Fig. 3, ΔT_i represents uncertainty in temperature due to uncertainty in model parameter i (the right term of Eq. (9)). It can be seen that the maximum value of ΔT_k increases from 9.8 K after 1 min of freezing, to 10.5 K after 10 min of freezing. At the same time, the maximum value of

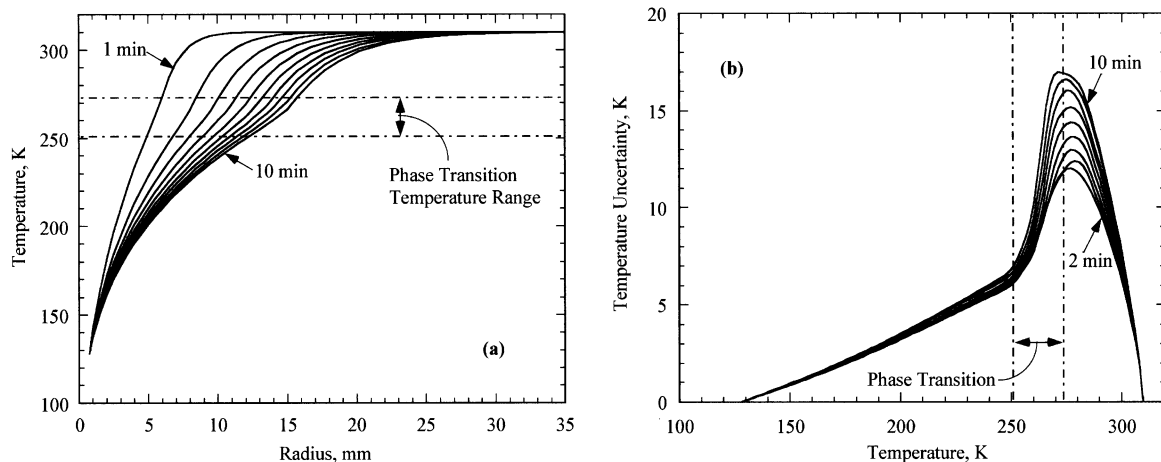


Fig. 2. Mathematical solution of temperature distribution around a cylindrical cryosurgical probe (a), and the corresponding estimation of uncertainty (b).

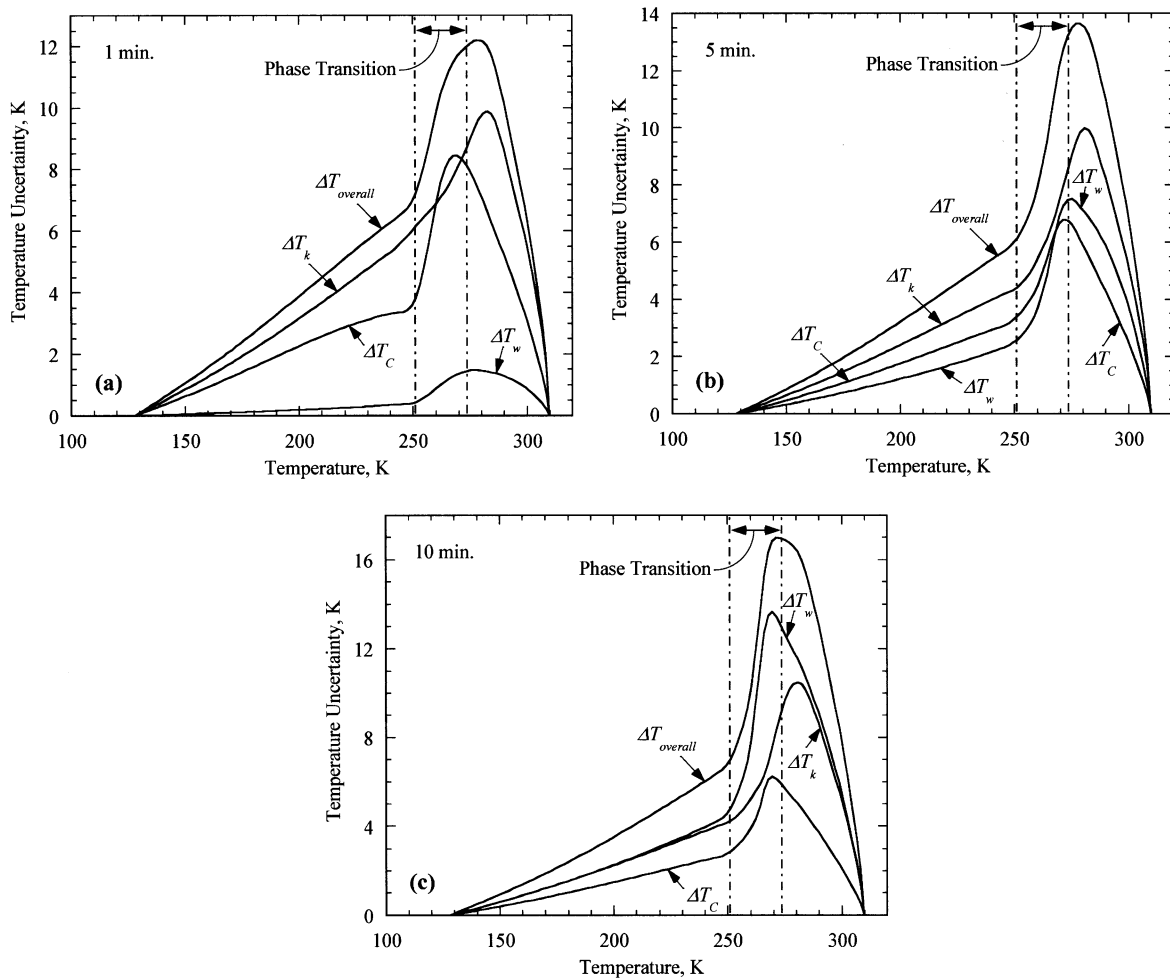


Fig. 3. Uncertainty in temperature at (a) 1 min, (b) 5 min, and (c) 10 min from the beginning of freezing. ΔT_i represents the absolute temperature difference between the solution based on average properties, and a solution based on a variation in property i only. The overall uncertainty is calculated using Eq. (5).

ΔT_k in the frozen region decreases from 6 to 4.2 K, respectively. It can be seen that the maximum value of ΔT_C decreases from 8.8 K after 1 min of freezing, to 6.2 K after 10 min of freezing. At the same time, the maximal value of ΔT_C in the frozen region decreases from 3.6 to 2.8 K, respectively. The maximum value of ΔT_w increases almost linearly with time, from a value of 3 K after 1 min of freezing, to a value of 13.6 K after 10 min of freezing. In fact, the linear increase in the maximum uncertainty value in Fig. 2(b) is mainly attributed to the linear increase in ΔT_w . The maximum value of ΔT_w in the frozen region also

increases almost linearly with time, from a value of 0.8 K after 1 min of freezing, to a value of 4.7 K after 10 min of freezing. The observation that the uncertainty in temperature is linearly dependent on the uncertainty in blood perfusion is consistent with the underlying assumptions of the mathematical formulation presented above. It can be seen from Fig. 3 that an extremely high uncertainty value of blood perfusion of 100%, leads to as much as 7.5% of uncertainty in the calculated temperature (13.6 K divided by the maximal temperature range of 128 and 310 K, and multiplied by 100).

For the purpose of discussion, the numerical example is now modified to include experimental observations. For this purpose, the following additional assumptions are made: (i) the purpose of the numerical simulation is to correlate the temperature distribution with histo-pathological findings, seeking the so-called lethal temperature; (ii) the experimental setup can be accurately modeled using the previous numerical example, i.e., 1D in a cylindrical geometry; (iii) the pathologist who analyzed the histology cross-sections identified a well defined edge of cryodestruction region at a radius R , with an uncertainty in measurements of ± 0.5 mm; and (iv) the computer simulation predicts 228 K (or, -45°C) at the exact same location, R . In other words, the -45°C isotherm appears to be the lethal temperature threshold in the hypothetical experiment. Fig. 4 presents the uncertainty in estimation of the lethal temperature value for the location identified by the pathologist, where R is the studied parameter. The radius R ranges from 2.4 to 8.4 mm in Fig. 4, which corresponds to the correlated location of the 228 K isotherm, from 30 s to 10 min of freezing, respectively. In the latter

case, the uncertainty in histology measurements is taken into account as:

$$\pm \frac{\partial f}{\partial p_i} \delta p_i = \pm \frac{\partial T}{\partial R} \delta R \quad (13)$$

in a similar way to the one presented in Eqs. (4) and (5).

It can be seen from Fig. 4 that the uncertainty in estimating the lethal temperature at the radius indicated by the pathologist, decreases monotonically with the increase in radius, from a range of 22.3 K after 30 s, to a range of 6.1 K after 10 min of freezing. It can further be seen that all sources of uncertainty taken into account in this study have a similar magnitude after 10 min of freezing. This observation has an impact on experimental design, where, for example, the lethal temperature analysis based on a larger frozen region is expected to be significantly more accurate.

Based on the results shown in Fig. 4, the worst case scenario can be estimated by the arithmetic sum of all individual uncertainties ΔT_i (excluding $\Delta T_{\text{overall}}$). It follows that the worst case scenario leads to an uncertainty level which ranges from 31.1 K after 30 s, to 12.2 K after 10 min of freezing. Note that the uncertainty level based on the worst case scenario is double the uncertainty level based on the formulation suggested in the current report after 10 min. Furthermore, the worst case scenario approximation shown in Fig. 4 is a conservative one, and presented here for the purpose of discussion only. By trial-and-error sensitivity analysis, one may find a set of model parameters leading to a much more severe worst case scenario than that presented in Fig. 4, all within the same estimated range of the uncertainty for the individual model parameters.

The computer simulation is given for a 1D case. Uncertainty analysis based on a 1D case defines the lower limit of uncertainty when compared with the full 3D case. The reason is that temperature gradients in a 3D case are steeper. It follows that a similar uncertainty in location of measurements in the 3D case leads to a higher uncertainty in the simulated temperature at the location of interest. Other reasons are associated with difficulties in measuring the precise location of measurements in a 3D experimental setup.

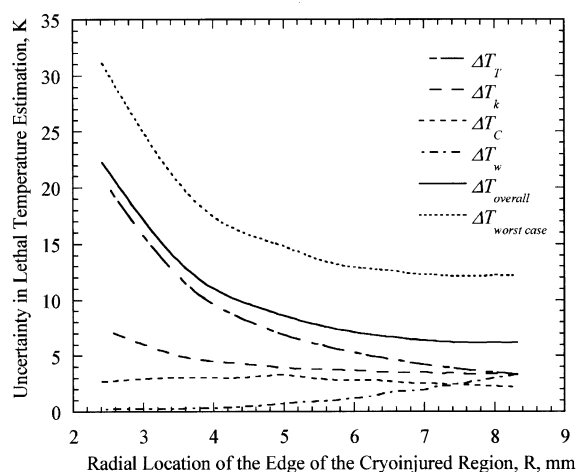


Fig. 4. Uncertainty in estimation of the lethal temperature value around a predicted average value of -45°C (228 K) in a 1D case. R is the radial location of an assumed edge of the cryoinjured region, where the uncertainty associated with R measurements is 0.5 mm. $\Delta T_{\text{overall}}$ represents the overall uncertainty using Eq. (5), while $\Delta T_{\text{worst case}}$ represents the worst case scenario, by summing the absolute value of all ΔT_i presented in the figure.

The mathematical formulation presented above is suitable for estimation of propagation of experimental uncertainties into computer simulations, when the functional behavior of each model parameter is known. However, this formulation is not suitable for analysis of uncertainty associated with modeling itself. For example, the current formulation cannot provide a systematic way to estimate uncertainty in computer simulation, due to uncertainty in the functional behavior of the latent heat. In the course of developing data for the current report, two functional behaviors of the latent heat have been considered, the first associated with a uniformly distributed effective specific heat, and the second behavior an ideal triangular shape, as illustrated in Fig. 1(c). Results presented in Figs. 1–4 are based on a uniformly distributed effective specific heat. Results based on an ideal triangular shape showed maximum temperature differences of less than 0.7 K in uncertainty analyses, which is deemed insignificant in the current study. However, this value of 0.7 K cannot be taken into account in Eqs. (1)–(10). This difference in temperature is likely to be related to numerical discretization, and not to the functional behavior of the latent heat [15].

Rabin and Korin [15] have shown that the specific numerical technique used in the current report inherently conserves energy. They have also shown that a typical difference between results of the current numerical technique and exact solutions of classical mathematical problems is measured in the order of 0.1% or less, which is translated to 0.1 °C or less in the current report. Comparison with other numerical techniques is also presented there. The reported study by Rabin and Korin [15] has been performed more than a decade ago on a 16 bit machine having an 8 MHz microprocessor and 640 KB of computer memory. Under those conditions, the numerical simulation had to be pushed to the limits of stability with a coarse mesh, in order to obtain results. Numerical results for the current report were generated on a 32 bit machine having a 1 GHz microprocessor and 512 MB of computer memory. The new conditions allow for fine mesh and significantly smaller time intervals than those required by stability criteria. The current computer parameters lead to a higher accuracy in numerical

results in orders of magnitude. It is noted that the numerical technique presented by Rabin and Korin [15] is a very expensive technique in terms of computer resources, with a resulting exceptionally low uncertainty. It is concluded that the effect of numerical uncertainty on the mathematical simulation is overwhelmed by the effects of experimental uncertainty of the model parameters.

Finally, all data presented in this report are based on a forward numerical formulation of derivatives in f , Eq. (9). Alternatively, the derivative of f could be based on a backward numerical formulation. There is no apparent reason why a forward formulation is superior to a backward formulation, or vice versa. Either way, similar uncertainty values are found, as long as either the uncertainty level of the model parameters is small, or when the resulted uncertainty in temperature is linearly dependent on the uncertainty in the model parameter.

Summary and conclusions

This report presents a concept for estimating the propagation of measurement uncertainties into a mathematical solution of bioheat transfer, which can be considered as an extension of the well-known concept of the rule of the square root of the sum of the square errors. Three elements are required in order to simulate heat transfer in a specific problem: (i) a thermal model of heat transfer, most commonly presented in the form of a differential equation (integral and lumped formulations are well established alternatives); (ii) a numerical technique for translating the thermal model into a numerical scheme; and (iii) a list of numerical values for all the thermal model parameters, as listed in the introduction. In this study, it was assumed that the thermal model and the functional behavior of all model parameters are known. This study is not dependent on a specific numerical technique. This report includes a method for the application of the new concept, which requires n consecutive numerical solutions, where n is the number of model parameters associate with a significant uncertainty in measurements.

A typical case of cryosurgery was analyzed, simulating an Argon cryoprobe in a 1D heat

transfer process. It was found that, in general, the uncertainty in temperature in the frozen region increases almost linearly with temperature, up to a value of 7 K after 10 min of simulation. The level of uncertainty in the unfrozen region increases almost linearly with time, from 12 K after 1 min to 17 K after 10 min of freezing. A linear dependency of the uncertainty in temperature on blood perfusion has been identified in the unfrozen region, which has a minor effect on the calculated temperature in the frozen region.

An advanced numerical example has been considered, in which computer simulations are used to estimate the lethal temperature value. It has been shown that prediction of the lethal temperature of -45°C (228 K) is likely to be associated with uncertainty interval ranging from 22.3 K after 30 s to 6.2 K after 10 min of freezing, while the frozen region developed to a diameter of 32 mm. Finally, the worst case scenario analysis is likely to predict much higher uncertainty analysis, by at least a factor of two, after 10 minutes of simulation.

In conclusion, it is highly recommended that the current technique for uncertainty analysis be used routinely when presenting computerized results, whether as a part of theoretical analysis, or in comparison with experimental data.

References

- [1] P.L. Altman, D.S. Dittmer, Respiration and circulation, Federation of American Societies for Experimental Biology (Data Handbook), Bethesda, MD, 1971.
- [2] B. Carnahan, H.A. Luther, J.O. Wilkes, Applied Numerical Methods, Wiley, USA, 1969.
- [3] C.K. Charny, Mathematical models of bioheat transfer, in: J.P. Hartnett, T.F. Irvine, Y.I. Cho (Eds.), Advances in Heat Transfer, Academic Press, New York, 1992, pp. 19–156.
- [4] J.C. Chato, Selected thermophysical properties of biological materials, in: A. Shitzer, R.C. Eberhart (Eds.), Heat Transfer in Biology and Medicine, Plenum Press, NY, 1985, pp. 413–418.
- [5] K.R. Diller, Modeling of bioheat transfer processes at high and low temperatures, in: J.P. Hartnett, T.F. Irvine, Y.I. Cho (Eds.), Advances in Heat Transfer, Academic Press, New York, 1992, pp. 157–358.
- [6] A.K. Datta, Biological and Bioenvironmental Heat and Mass Transfer, Marcel Dekker, USA, 2002.
- [7] S. Fukusako, Thermophysical properties of ice, snow, and sea ice, *Int. J. Thermophys.* 11 (2) (1990) 353–372.
- [8] A.A. Gage, J. Baust, Mechanisms of tissue injury in cryosurgery, *Cryobiology* 37 (3) (1998) 171–186.
- [9] J.P. Holman, Experimental Methods for Engineers, seventh ed., McGraw-Hill, New York, 2001.
- [10] R. Kuzman, Handbook of Thermodynamics and Tables, McGraw-Hill, New York, 1976.
- [11] J.R. Mahan, Radiation Heat Transfer: A Statistical Approach, Wiley, New York, 2002.
- [12] P. Mazur, S. Leibo, E.H.Y. Chu, A two-factor hypothesis of freezing injury, *Exp. Cell Res.* 71 (1972) 345–355.
- [13] W.H. Newman, P.P. Lele, A transient heating technique for the measurement of thermal properties of perfused biological tissues, *ASME J. Biomech. Eng.* 107 (1985) 219–227.
- [14] H.H. Pennes, Analysis of tissue and arterial blood temperatures in the resting human forearm, *J. Appl. Phys.* 1 (1948) 93–122.
- [15] Y. Rabin, E. Korin, An efficient numerical solution for the multidimensional solidification (or melting) problem using a microcomputer, *Int. J. Heat Mass Trans.* 36 (3) (1993) 673–683.
- [16] Y. Rabin, R. Coleman, D. Mordohovich, R. Ber, A. Shitzer, A new cryosurgical device for controlled freezing, part ii: in vivo experiments on rabbits' hind thighs, *Cryobiology* 33 (1996) 93–105.
- [17] Y. Rabin, Uncertainty in measurements of fluid temperature in tubes, *Cryo-Letters* 19 (5) (1998) 319–326.
- [18] Y. Rabin, Uncertainty in temperature measurements during cryosurgery, *Cryo-Letters* 19 (4) (1998) 213–224.
- [19] Y. Rabin, A. Shitzer, Numerical solution of the multidimensional freezing problem during cryosurgery, *ASME J. Biomech. Eng.* 120 (1) (1998) 32–37.
- [20] Y. Rabin, The effect of temperature-dependent thermophysical properties in heat transfer simulations of biomaterials in cryogenic temperatures, *Cryo-Letters* 21 (2000) 163–170.
- [21] Y. Rabin, T.F. Stahovich, Cryoheater as a means of cryosurgery control, *Phys. Med. Biol.* 48 (2002) 619–632.
- [22] A. Shitzer, On the relationship between temperature, blood flow, and tissue heat generation, in: A. Shitzer, R.C. Eberhart (Eds.), Heat Transfer in Biology and Medicine, Plenum Press, New York, 1985, pp. 395–409.
- [23] A. Shitzer, R.C. Eberhart (Eds.), Heat Transfer in Biology and Medicine, Plenum Press, New York, 1985.
- [24] J.D. Smith, R.V. Devireddy, J.C. Bischof, Prediction of thermal history and interface propagation during freezing in biological systems—Latent heat and temperature-dependent property effects, in: Proceedings of the 5th ASME/JSME Joint Thermal Engineering Conference, San Diego, CA, AJTE, 1999, pp. 99–6520.
- [25] J.W. Valvano, J.T. Allen, H.F. Bowman, The simultaneous measurement of thermal conductivity, thermal diffusivity, and perfusion in small volumes of tissue, *ASME J. Biomech. Eng.* 106 (1984) 192–197.